

Conf-820822--7

UCRL 87363
PREPRINT

UCRL--87363

DE82 020168

THE APPLICATION OF FAST INFRARED DETECTORS
TO DETONATION SCIENCE

NOTICE

W. G. Von Holle
R. A. McWilliams

PORTIONS OF THIS REPORT ARE ILLEGIBLE. IT

**has been reproduced from the best available
copy to permit the broadest possible avail-
ability.**

This paper was prepared for submittal
to the 26th International Technical
Symposium, San Diego, CA.
August 22-27, 1982

July 28, 1982

MASTER

Lawrence
Livermore
Laboratory

The application of fast infrared detectors to detonation science*

William G. Von Holle and Roy A. McWilliams

Lawrence Livermore National Laboratory, Chemistry and Materials Science Department,
University of California, Livermore, California 94550

Abstract

Infrared radiometers have been used to make time-resolved emission measurements of shocked explosives. Instruments of moderate time resolution were used to estimate temperatures in shocked but not detonated explosives. The heterogeneity of the shock-induced heating was discovered in pressed explosives by two-band techniques, and the time-resolved emittance or extent of hot spot coverage indicated a great dependence on shock pressures. Temperatures in moderately shocked organic liquids were also measured.

Faster response radiometers with 5 ns rise times based on InSb and HgCdTe photovoltaic detectors were constructed and tested. Preliminary data on reactive shocks and detonations reveals a resolution of the heating in the shock wave and the following reaction.

Introduction

The application of time resolved infrared radiometry to detonation related phenomena occurred first with the temperature measurement of shocked metal plates^{1,2,3} and shaped charge jets³ in flight. Mid-infrared detectors such as InSb are convenient for these problems in which the temperature range encountered is 200 to 1500°C. Visible and ultraviolet pyrometry, which are well developed techniques in many laboratories, are best suited to higher temperature hydrodynamic phenomena. They will not be discussed in this paper.

It seemed reasonable to extend the infrared techniques developed in the work on metals to the detection of the energy liberated by chemical reactions induced by shock waves in organic energetic materials. One expects chemical decomposition reactions to begin at about 200°C in many explosives and propellants, and, of course, final temperatures achieved are potentially much higher, depending on the kinetics and thermodynamics of the particular reactions in specific materials.

Time-resolved infrared radiometry has become a useful new technique for the characterization of the sensitivity of explosives and propellants to detonation by shockwaves. This paper is an update on the highlights of this application in several different experiments which are of interest to the detonation community and which demonstrate a unique application of fast infrared detection. The first part will be a review and brief description of significant new results obtained with the 400 ns radiometers followed by a discussion of the current efforts with a new set of fast-rise instruments.

Experimental -- Instrumentation

Originally, the work done at Livermore on the measurement of the infrared emission from shocked energetic materials was done with radiometers converted from line scanners made by Inframetrics, Corp., Bedford, Massachusetts. They contained InSb detectors, 2-5.5 μm , with an approximate D^* of 1.1×10^{11} $\text{cm}^2/\text{Hz}^2 \text{ watt}^{-1}$ and a fixed instantaneous field of view of 2×10^{-3} radian. For most applications a sharp cut-on filter at 4.086 μm was used on one detector in a pseudo two-color system with a 2 mm-thick sapphire beam splitter. Calibration was performed in the actual experimental configuration with a 200-1000°C infrared blackbody source. Experiments on 20 ns pulsed laser burn of aluminized mylar films indicated a response time of less than 500 ns.

Much faster risetime radiometers incorporating InSb (2-5.5 μm) and HgCdTe (5.5-11.3 μm) detectors from Eltek, Corp., Larchmont, N.Y., were designed and constructed in-house. Both of these were similarly designed with Perry Model 490 wideband signal amplifiers and 100 mm f.l., 50 mm diameter Germanium lenses for focusing. Details of the construction and testing will be found in reference 4. Figure 1 shows a labeled photograph of one of the fast radiometers, which have instantaneous fields of view of less than 3×10^{-3} radians. The translatable lens allows variable focusing, but it has only been used at a constant range of of 1.3 m. A 101 mm single-stage gas gun was used to launch projectile flyer plates in order to produce smooth, flat shock waves in the samples. Figure 2 shows the

*Work performed under the auspices of the U.S. Department of Energy by the Lawrence Livermore National Laboratory under contract No. W-7405-ENG-48.

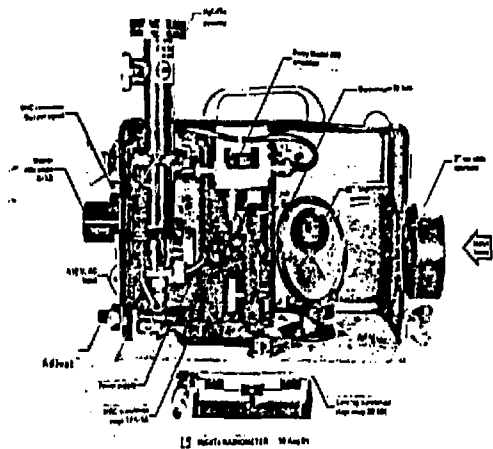


Figure 1. Photo of fast HgCdTe radiometer with cover removed.

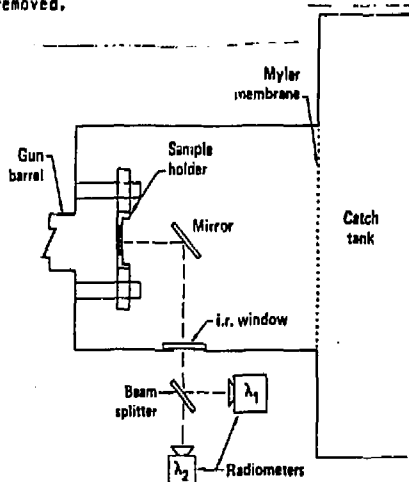


Figure 2. 101 mm gun experimental arrangement.

experimental arrangement used with the gun. Piezoelectric pins were used to determine projectile velocity, tilt and to trigger recording oscilloscopes. Most experiments were carried out with 7 or 12 mm thick flyers of Aluminum or Copper, and their velocities were varied to vary the impact shock pressure in the samples. Ambient pressure in the experimental chamber was always less than 50 milli-Torr at shot time.

Results and discussion -- Opaque explosives

In the first experiment done on the measurement of the infrared emission from shocked explosives, a 5 mm thick disk of shocked PBX9404** yielded the radiance histories in Figure 3. The signal peaks near the beginning are evidence for the formation and cooling of small hot spots near the free surface of the explosive. In support of this contention, the ratio of two band temperature at the peak is considerably greater than either single-band result, and the nearly exponential decay from the peak with an approximate 10 μ s time constant is indicative of an initial hot spot size on the order of few microns.⁵ Consistent with this interpretation, similar experiments on low density and high porosity explosives yielded higher radiances and temperatures, as expected, and a large effect of particle size distribution.⁶

Bare charges of the insensitive explosive TATB, (triaminotri-nitrobenzene) were shocked in experiments similar to the HMX-containing materials with results as shown in Figure 4. The 2-5.5 μ m band signal history shape is similar to PBX9404 except that the peak signal level is considerably smaller; however, the 4-5.5 μ m peak is nearly flat. This non-grey body behavior could be explained by the nature of the hot spots in TATB. Perhaps the cause is a lack of chemical reactivity in cooler hot spots in which only the hot TATB emits with little of the final combustion products, H₂O and CO₂, present. The 4-5.5 μ m region encompasses strong absorption (and emission) bands of H₂O and CO₂ only, without strong TATB bands, while the 2-5.5 μ m band is sensitive to both hot TATB and products of complete composition reaction.⁷

Although the above bare charge results have been useful in the study of shock-induced reactivity, a lack of knowledge of shock-released surface states leaves us without quantitative information. In these experiments the material near the free surface is shocked and immediately released by the rarefaction from the surface. In order to

** 94% cyclotetramethylene tetranitramine (HMX), 4% nitrocellulose and 3% Tri-chlorethylphosphate plus stabilizer.

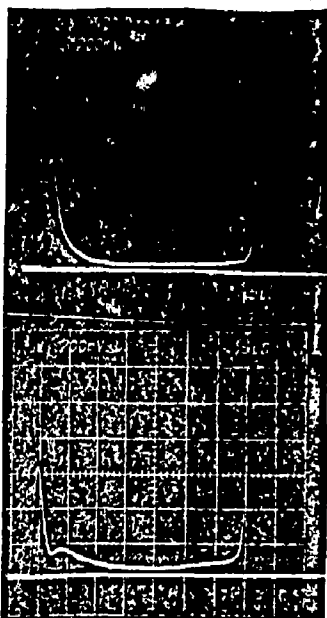


Figure 3. Oscilloscope traces from a 3.8 GPa impact on 5 mm thick bare PBX 9404. The top trace is the 2-5.5 μ m band; the lower is the 4-5.5 μ m band. Both are 5 μ s per major division sweep speed.

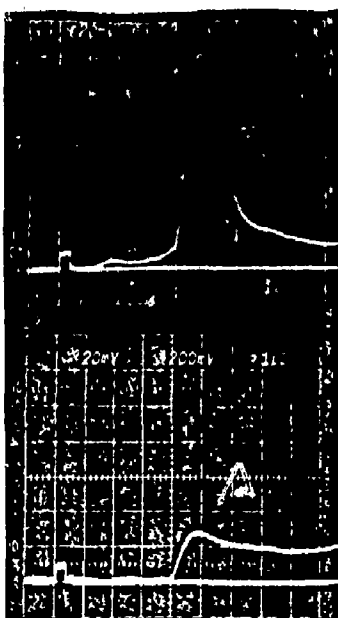


Figure 4. Oscilloscope traces from a 8.0 GPa impact on 12.7 mm thick bare TABT. The top trace is the 2-5.5 μ m band; the lower is the 4-5.5 μ m band. Both are 1 μ s per major division sweep speed.

simulate the interior of the explosives hydrodynamically, shock impedance-matching infrared transmitting windows were attached to their down-stream faces. As long as the window is a good impedance match, the pressure is sustained and the thermodynamic state of a finite thickness of material observed near the interface evolves as if the window were not present at least until a rarefaction reaches the interface. Thermal conduction is negligible on the time scale of these experiments. Figure 5 shows a comparison of the two techniques with an HMX containing propellant. Addition of the window causes an immediate, strong reaction following shock passage while the bare charge exhibits only an initial weak signal followed much later by a stronger signal.

As in the bare charge case, a large discrepancy between the single band and two-band or color temperatures was discovered. Again, the color temperatures were much higher than the single band results, indicating a heterogeneously heated explosive material. In addition, the evolution of this surface could now be monitored with some knowledge of the hydrodynamic state of the material. The emittance in each band was calculated according to equation 1.

$$\epsilon_{\text{band}} = \frac{w_{\text{obs}}}{\int w_{\text{bb}}(\lambda, T) d\lambda} \quad (1)$$

In equation (1), w_{obs} is the observed signal, $w_{\text{bb}}(\lambda, T)$ is the Plank blackbody function, and the integral is the single-band radiance at the true temperature. The band emittance can be considered as a measure of the surface fraction of explosive reacted under certain assumptions. The most important ones are that the emittance of the hot spots themselves is unity and that the surrounding material is relatively cooler. Resultant fraction reacted histories for several experiments on PBX9404/KCl are shown in Figure 6. For these results the average of the two-band temperatures, which remained relatively independent of impact shock pressures, was assumed to be the true temperature. Creditability of the results rests mainly on a close match by a simulation with a computer calculation using a 1D hydro-code including a pressure dependent energy release rate⁸ and a near coincidence for the two independently obtained single bands. Two interesting features of these fraction reacted histories are the rapid change of slope (reaction rate)

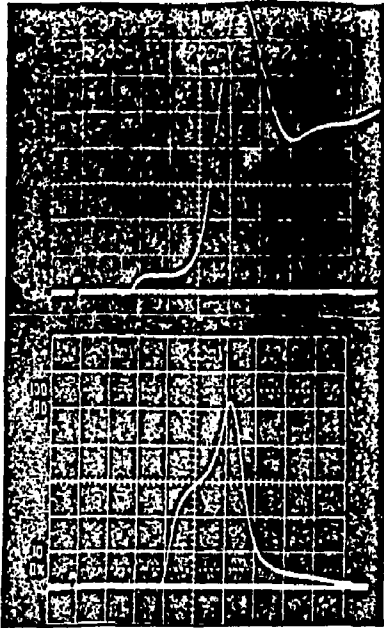


Figure 5. Comparison of two experiments on an HMX-based propellant. The top trace is the 2-3.5 μm band result from the bare material at 3.0 GPa; the bottom from the same propellant with KCl attached at 2.75 GPa

embedded manganin pressure gauge experiments,⁹ in which the pressure increases very rapidly following shock passage for moderately strong shocks. The similar appearance of the manganin pressure histories and the radiance curves indicates a moderate effect of pressure on the rate of reaction following a given shock. Figure 7 illustrates the extreme dependence of the initial reaction rate on shock pressure for various experiments. The straight line fit to the data shown in the figure is a power law with an exponent of 6.7. Undoubtedly, some integration over the response time of the radiometers and a non-zero i.r. penetration depth added some contribution to the exponent, but there remains a sharp dependence. From this we concluded that the number of hot spots per unit area is greatly dependent on shock strength, establishing a clear experimental distinction between the hot spot formation process and their subsequent growth.⁶

Recent work on the TATB/KCl system shows a similar dependence of the fraction reacted histories on impact pressure. In this case, however, a large effect of particle size distribution was also discovered. Figure 6 shows reaction histories from two sets of experiments, one using an ultrafine particle size distribution (mean size, 9 μm) and one a much coarser distribution (mean size 58 μm); each was pressed to the same nominal density, 1.86 g/cm³. Within each set of experiments, increasing impact pressure causes large changes in the reaction curves. Also, there are two outstanding differences due to particle distribution shown in Figure 6. The first is that the signals arise sooner in the coarse material, implying that the shock velocity is higher in this material. Secondly, the initial slopes of the curves (reaction rates) are greater in the fine TATB for similar impact shock strengths. Comparisons at the shock pressures near 5.1 GPa and 7.5 GPa are the most revealing. At first these two observations may seem contradictory; however, one must distinguish between reaction in or near the shock front, which would most affect the velocity, and reaction following the front. The results could be interpreted by hotter hot spots in the coarse than in the fine explosive, which experiences a higher burn rate later in the flow due to a larger number of hot spots and a larger specific surface area. These conclusions are preliminary and await further experimental corroboration, but they are consistent with our earlier interpretation of the PBX 9404 fraction reaction histories, namely, that a larger initial slope means a larger number of hot spots.

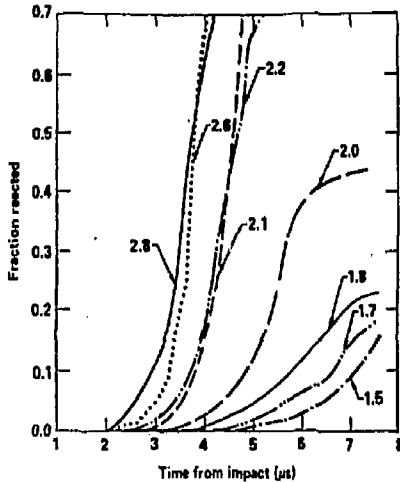


Figure 6. PBX 9404/KCl fraction reacted histories. Numbers refer to the impact pressure in GPa.

with time for each experiment and the great sensitivity of the initial slopes to impact shock pressure.

The first feature is consistent with

the similar appearance of the manganin pressure histories and the radiance curves indicates a moderate effect of pressure on the rate of reaction following a given shock. Figure 7 illustrates the extreme dependence of the initial reaction rate on shock pressure for various experiments. The straight line fit to the data shown in the figure is a power law with an exponent of 6.7. Undoubtedly, some integration over the response time of the radiometers and a non-zero i.r. penetration depth added some contribution to the exponent, but there remains a sharp dependence. From this we concluded that the number of hot spots per unit area is greatly dependent on shock strength, establishing a clear experimental distinction between the hot spot formation process and their subsequent growth.⁶

Recent work on the TATB/KCl system shows a similar dependence of the fraction reacted histories on impact pressure. In this case, however, a large effect of particle size distribution was also discovered. Figure 6 shows reaction histories from two sets of experiments, one using an ultrafine particle size distribution (mean size, 9 μm) and one a much coarser distribution (mean size 58 μm); each was pressed to the same nominal density, 1.86 g/cm³. Within each set of experiments, increasing impact pressure causes large changes in the reaction curves. Also, there are two outstanding differences due to particle distribution shown in Figure 6. The first is that the signals arise sooner in the coarse material, implying that the shock velocity is higher in this material. Secondly, the initial slopes of the curves (reaction rates) are greater in the fine TATB for similar impact shock strengths. Comparisons at the shock pressures near 5.1 GPa and 7.5 GPa are the most revealing. At first these two observations may seem contradictory; however, one must distinguish between reaction in or near the shock front, which would most affect the velocity, and reaction following the front. The results could be interpreted by hotter hot spots in the coarse than in the fine explosive, which experiences a higher burn rate later in the flow due to a larger number of hot spots and a larger specific surface area. These conclusions are preliminary and await further experimental corroboration, but they are consistent with our earlier interpretation of the PBX 9404 fraction reaction histories, namely, that a larger initial slope means a larger number of hot spots.

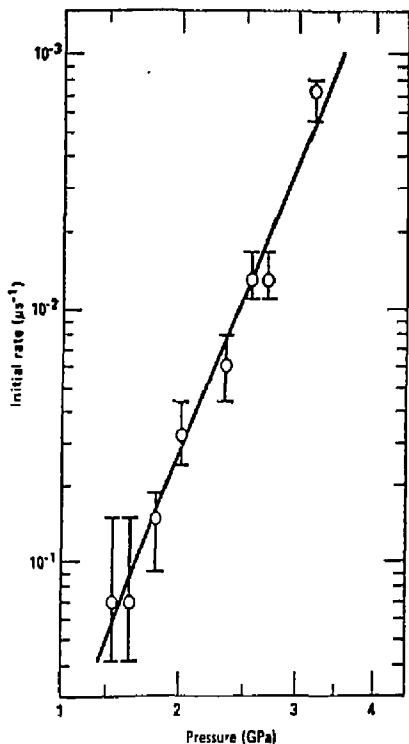


Figure 7. PBX 9404/KCl initial slope of fraction reacted histories (rates) versus impact pressure.

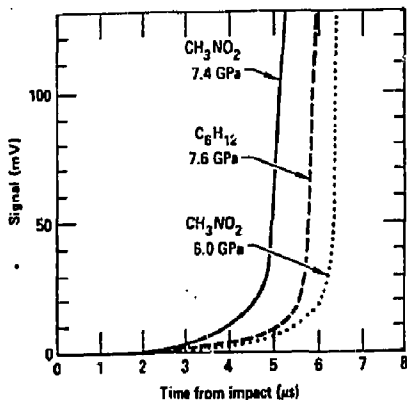


Figure 9. 2-5.5 μs signals from three experiments on neat liquids, which were contained between polished stainless steel buffer plates and 2.0 mm thick sapphire windows.

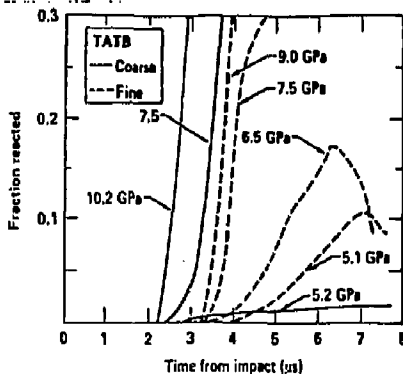


Figure 8. TATB/KCl fraction reacted histories. Numbers refer to impact pressures.

Shocked liquid temperature measurements

Temperature measurements in shocked organic liquids are important because of the theoretical difficulty of calculating accurate temperatures and because of their importance in the interpretation of shocked liquid explosives. Time-resolved infrared radiometry offers a non-intrusive, remote technique for such measurements which is particularly attractive.

Figure 9 shows the early radiance signal histories from three typical experiments on two liquids of about 21 mm thickness with a sapphire window. These are clearly different from the opaque solid results. An exponential increase is followed by a sharper rise, presumably at shock impact with the sapphire window. The following interpretation allows the determination of Hugoniot temperatures for moderate shocks. Solution of the radiation transport equation¹⁰ modified for a shock in a partially transparent homogeneous medium, assuming the reflectivities of the shock front and buffer (driver) plate are negligible, leads to an expression for the observed radiation, w_{obs} , in equation 2

$$w_{obs} = \int (1 - T(\lambda)) e^{-a x} w^{bb}(\lambda, T) d\lambda \quad (2)$$

where $T(\lambda)$ is the transmittance of the shocked layer; a is the absorption coefficient of the remaining unshocked liquid of thickness, x ; and $w^{bb}(\lambda, T)$ is the Planck blackbody function, as before. Equation 2 reduces to an exponential dependence of the radiance signal on x (or time) as $T(\lambda)$ approaches zero, in agreement with the observed

exponential signals of Figure 9. When $x = 0$ in equation (2), i.e., the shock reaches the end of the liquid, the observed signal should correspond to the blackbody value. Results of several experiments on nitromethane, a very insensitive liquid explosive, yielded reasonable temperatures which were similar for each band below 7.0 GPa.¹¹ At 7.4 GPa significant deviations between the two bands occurred; the signal levels increased above that expected for an inert shock for the 7.4 GPa nitromethane curve as in Figure 9. It is believed that an unexpected partial decomposition reaction occurring before detonation is the cause for the deviation in behavior of nitromethane above 7.0 GPa.

Results of 5 ns radiometers

As a demonstration of the rise time of the fast response radiometers and as a dynamic calibration of the new instruments, experiments were done on a previously examined system, explosively loaded copper plates. Figure 10 is an oscilloscope trace of the voltage from the InSb radiometer looking at a 1.5 mm copper plate driven by detonating PBX 9404. The plate was polished flat then oxidized in a furnace to increase the infrared emissivity. The observed rise time of about 10 ns must be reduced by about 5 ns tilt in the impacting flyer over the 4 mm spot size, leaving approximately 5 ns for the detector-electronics contribution to the rise time. The expected flat signal from the residual temperature of the target persists over the length of the trace with the desired signal-to-noise ratio. A similar fast rise was observed for the HgCdTe radiometer in a separate experiment.

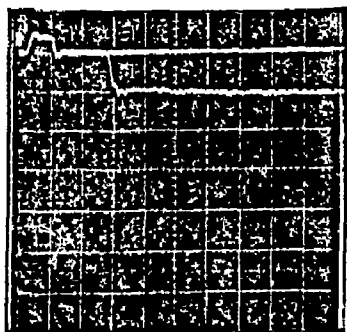


Figure 10. Oscilloscope trace of an explosively loaded 1.5 mm thick oxidized copper plate by the InSb detector with a negatively going signal. Sweep rate is 50 ns per large division.

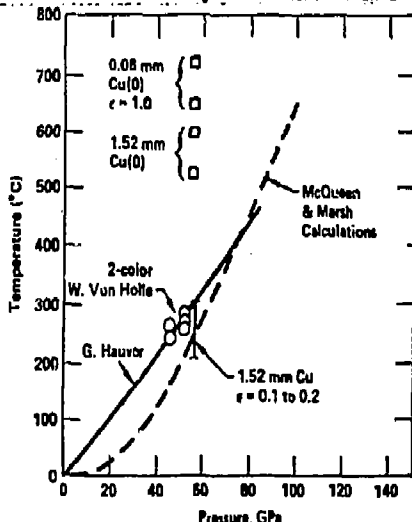


Figure 11. Experimental and calculated copper residual temperatures.

Much lower signals were observed with shocked polished OFHC copper plates, but the results can be compared to previous experimental and calculated copper residual temperatures. Figure 11 contains the current residual temperatures of shocked, mirror-polished plates and the oxidized plates. The abscissa is the approximate pressure generated in the metal by the explosive loading. These results on polished copper, which is shown as the range for a range of the assumed emittance, were obtained from the InSb and HgCdTe instruments in separate experiments. The new data range spans past experimental values obtained from two-color infrared radiometry,² resistance measurements of explosively loaded copper foils¹² and the calculated values.¹³ The oxidized copper plate data, labeled Cu(O) in the figure and derived using an emittance of unity, lie understandably at higher temperatures.

The results of a shocked TATB (1.86 g/cm³) experiment is contained in Figure 12. For these experiments, the 12.7 mm disks of ultrafine TATB were polished flat and attached to KCl windows with a small amount of silicone grease to insure a continuous interface. The earlier TATB/KCl results were obtained by pressing TATB powder directly onto KCl disks in a ram press. Radiance histories from the HgCdTe radiometer placed in the number one position (see Fig. 2) are shown in Figure 12. Reflection of a KCl beam splitter resulted in about a 90% degradation of signal-to-noise. In the trace from the higher impact pressure experiment a sharp increase near shock arrival at the interface is followed by a more gradual increase to a level signal. Preliminary interpretation is that the sharp

increase represents heating in the shock front which is followed by increasing levels of reaction. Radiance histories observed with the slow radiometers did not resolve this first feature, which allows a direct observation of the relative energy release in the shock and following! Lowering the impact pressure to 7.6 GPa, substantially reduces the shock wave front signal and nearly eliminates the following growth.

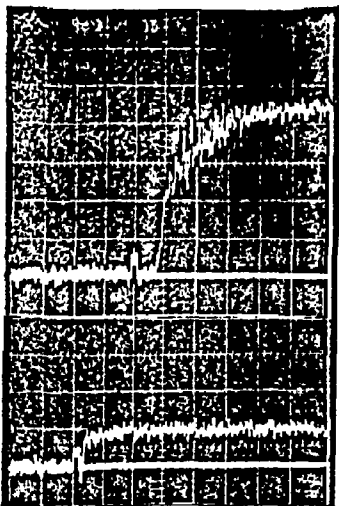


Figure 12. HgCdTe traces from shocked TATB experiments. Shock pressures were 9.0 GPa for the top and 7.6 GPa for the bottom. Both are 200 ns per major division.

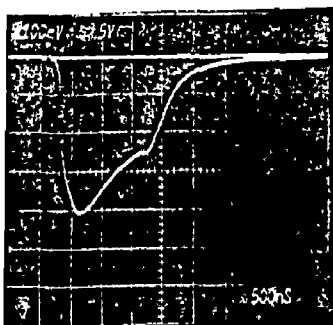


Figure 13. HgCdTe trace from a detonation in PBX 940A observed through-KBr at 500 ns per major division.

indicates a non-greybody emission with HgCdTe detector yielding a much higher peak temperature. More experiments and theoretical calculations are required to explore the potential of this new technique to reveal information on detonation reaction zone structure.

Conclusions

Infrared radiometry is a relatively new tool for reactive shock wave and detonation diagnostics, and applications are just beginning. Some have been reviewed in this paper, and many more are feasible. Beyond simple radiometry we look forward to new developments

Results from the InSb radiometer in position #2 indicate the same contrasting behavior between the two experiments. The observed threshold-like behavior is consistent with the previous set of results shown in Figure 8 for ultrafine TATB; however, the 7.5-7.6 GPa comparison between the two sets indicates disagreement as to the threshold pressure, probably because of the different interface preparation.

Quantitative analysis of the shocked TATB data has not yet been done, but the results thus far are encouraging. Additional experiments will be carried out at various impact pressures and with different particle size distributions.

Experiments on detonating explosives in similar target assemblies as the above shock studies revealed interesting radiance histories. A typical trace resulting from a detonation in PBX940A passing into a KBr window, which comes close to matching the 940A detonation product Hugoniot, is shown in Figure 13. Preliminary interpretation is based on the Zeldovitch-vonNeuman-Doring¹⁴ theory of reaction zone structure. Essentially it is a strong shock wave initiating chemical reaction which is complete at the Chapman Jouget (CJ) plane followed by the expanding and cooling detonation products. A short exponential signal increase is followed by a sharp increase of only a few nanoseconds duration, which is probably the result of the leading shock. The much slower rise to the peak signal and decrease may represent subsequent energy release in the reaction zone; however, the time to reach the peak signal is too long to represent the actual reaction zone thickness as measured by other techniques, e.g., 50 ns, measured by experimental particle velocity records.¹⁵

Other explosives yield similar data with different signal levels and different time intervals. Preliminary assignment of brightness temperatures

200-014

In infrared technology for future applications, such as gated or time- and wavelength-resolved multiplex detection and high resolution imaging in a single shot.

Acknowledgements

The authors thank the 101 mm gun crew, William Mumper, William Duguid and Melvin Bainter for their diligence in the many gun firings. A special recognition is given to Howard Whiting for his work on the electronics of the 5 ns radiometers and to Robert Reedy for his expert optical advice.

References

1. King, Cotgrove and Slate, "Behavior of Dense Media Under High Dynamic Pressures," Gordon and Breach, New York, 1968, pg. 513.
2. W. G. Von Holle and J. J. Trimble, *J. Appl. Phys.*, **47**, 2391, (1976).
3. W. G. Von Holle and J. J. Trimble, "Sixth Symposium (International) on Detonation," DNR, ACR-221, 1976, pg. 691.
4. W. G. Von Holle and R. McWilliams, to be submitted to *Rev. of Sci. Instruments*.
5. W. G. Von Holle and E. L. Lee, "Behavior of Dense Media under High Dynamic Pressure," Commissariat a l'Energie Atomique, Paris, France, 1978, pg. 425.
6. W. G. Von Holle, "Temperature Measurements of Shocked Energetic Materials by Time-Resolved Infrared Radiometry, in *Fast Reactions in Energetic Systems*, Eds: C. Capellos and R. Walker, D. Reidel, Boston, 1980, pg. 485.
7. T. G. Towns "Vibrational Spectrum of 1,3,5-Triamino-2,4,6-Trinitrobenzene," Lawrence Livermore National Laboratory Report UCRL 85914 (April, 1981).
8. W. G. Von Holle and C. M. Tarver, *7th Symposium (International) on Detonation*, Annapolis, Maryland, June 16-19, 1981.
9. R. Weingart, et. al., "Behavior of Dense Media under High Dynamic Pressures," Commissariat a l'Energie Atomique, Paris, France, 1978, pg. 451.
10. H. G. McMahon, *J. Op. Soc. Am.*, **40**, 376 (1950).
11. W. G. Von Holle in *Shock Waves in Condensed Matter - 1981* (Menlo Park) Eds: W. J. Nellis, L. Seaman and R. A. Graham, American Institute of Physics, New York, 1982, pg. 287.
12. G. Hauver, BRL, Aberdeen Proving Grounds, Maryland, unpublished results.
13. R. G. McQueen and S. P. Marsh, *J. Appl. Physics*, **31**, 1253 (1960).
14. For an explanation of the ZND theory, see, for example, W. Fickett and W. C. Davis, "Detonation," U. of California Press, Berkeley, CA., 1979.
15. B. Hayes and C. M. Tarver, *Seventh Symposium (International) on Detonation*, Annapolis, Maryland, June 16-19, 1981.

DISCLAIMER

This document was prepared as an account of work sponsored by an agency of the United States Government. Neither the United States Government nor the University of California nor any of their employees, makes any warranty, express or implied, or assumes any legal liability or responsibility for the accuracy, completeness, or usefulness of any information, apparatus, product, or process disclosed, or represents that its use would not infringe privately owned rights. Reference herein to any specific commercial products, process, or service by trade name, trademark, manufacturer, or otherwise, does not necessarily constitute or imply its endorsement, recommendation, or favoring by the United States Government or the University of California. The views and opinions of authors expressed herein do not necessarily state or reflect those of the United States Government thereof, and shall not be used for advertising or product endorsement purposes.